ELSEVIER

Engineering Geology 64 (2002) 157–178

ENGINEERING GEOLOGY

www.elsevier.com/locate/enggeo

Influence of pressurized water influx on the hygro-thermal behaviour of an engineered clay barrier in a waste emplacement borehole

A.P.S. Selvadurai *

Department of Civil Engineering and Applied Mechanics, McGill University, Montreal, Quebec, Canada H3A 2K6

Received 17 March 2000; accepted 13 July 2001

Abstract

This paper presents the results of a series of experiments conducted to examine the hygro-thermal behaviour of a compacted, internally heated engineered clay barrier, consisting of a mixture of bentonitic clay and sand, compacted in a laboratory scale model simulating a waste emplacement borehole located in a granitic rock. The experiments considered the supply of water at a prescribed pressure at the outer cylindrical and plane boundaries of the compacted, engineered clay barrier. The experiments examined the manner in which the water supply conditions influenced the extent of the moisture uptake within the compacted clay barrier. The experimental results presented in this paper include contours of the time-dependent variation of temperature within the granite block, the time-dependent variations of temperature at the midsection level of the internally placed heater and along the axis of the experimental facility, and the residual volumetric moisture content distribution determined at the termination of the experiments.

Keywords: Engineered geological barriers; Clay barriers; Pressurized moisture influx; Borehole emplacement; Hygro-thermal effects; Bentonite–sand buffer

1. Introduction

The Canadian proposals for the disposal of the heat-emitting radioactive wastes concentrate on their deep burial in the plutonic rock masses of the Canadian Shield (Johnson et al., 1994; Simmons and Baumgartner, 1994). The basic concepts advocated in these proposals are in keeping with the methodologies being proposed by other countries for the deep geological disposal of the heat-emitting highly radioactive wastes in the rock masses (Laughton et al., 1986; Chapman and McKinley, 1987; OECD, 1988; Gray, 1993; Gnirk, 1993; SKI, 1993; Huertas et al., 2000). Current concepts for these deep disposal facilities identify several important components, which are intended to serve as both the engineered and natural geological barriers for mitigating the long-term radionuclide migration. The vault system itself is constructed to a specific shape in a rock mass with known physical, mechanical, chemical, hydrogeological and tectonic characteristics; the rock mass serves as the primary natural geological barrier for the radionuclide migration. The primary engineered barrier

* Tel.: +1-514-398-6672; fax: +1-514-398-7361.
E-mail address: patrick.selvadurai@mcgill.ca (A.P.S. Selvadurai).

0013-7952/02/$ - see front matter
PII: S0013-7952(01)00105-3

involves the sealed cylindrical containers that house the heat-emitting radioactive waste. The primary engineered geological barrier is a highly dense mixture of the bentonitic clay and crushed quartz sand within which the waste containers are emplaced (Lopez, 1987; Graham et al., 1990; Selvadurai and Cheung, 1991; Selvadurai, 1990, 1996a,b). This engineered clay barrier, which in its compacted state is also referred to as a "buffer", is either compacted in situ in emplacement boreholes that are drilled into the base of the galleries of the waste disposal vault system or placed around the waste containers in pre-compacted units. The secondary engineered geological barrier is the backfill material that fills the major part of the waste disposal vault system. In addition, other engineered barriers, such as the backfilling of the access shafts and boreholes, the use of bulkheads for the shaft and borehole sealing, etc., form the complete system of engineered barriers intended to minimize the migration of radionuclides from the repository to the biosphere throughout the harmful life of the stored radioactive waste. A conceptual description of the engineered barrier system and its components of interest to the environmental geomechanics are shown in Fig. 1.

The use of bentonitic clays as engineered geological barriers is advocated in many concepts put forward for the deep disposal of the heat-emitting radioactive wastes (Come et al., 1985; Chapman and McKinley, 1987; Lopez, 1987; Ishikawa et al., 1989; Cheung, 1990; Pusch, 1990; SKI, 1993; Gray, 1993; Johnson et al., 1994; Hueckel and Peano, 1995; Fujita et al., 1997; Selvadurai, 1997; Gens et al., 1998; Jing et al., 1999; Stephansson et al., 2001). The potential for the bentonitic clays to act as geochemical filters for the sorption of radionuclides is an important factor in their choice as an engineered geological barrier. It is anticipated that such radionuclide migration cannot be prevented indefinitely, and will eventually occur as a result of the natural disintegration of the waste containers. The composition of the engineered clay barrier and the chemical characteristics of its constituents

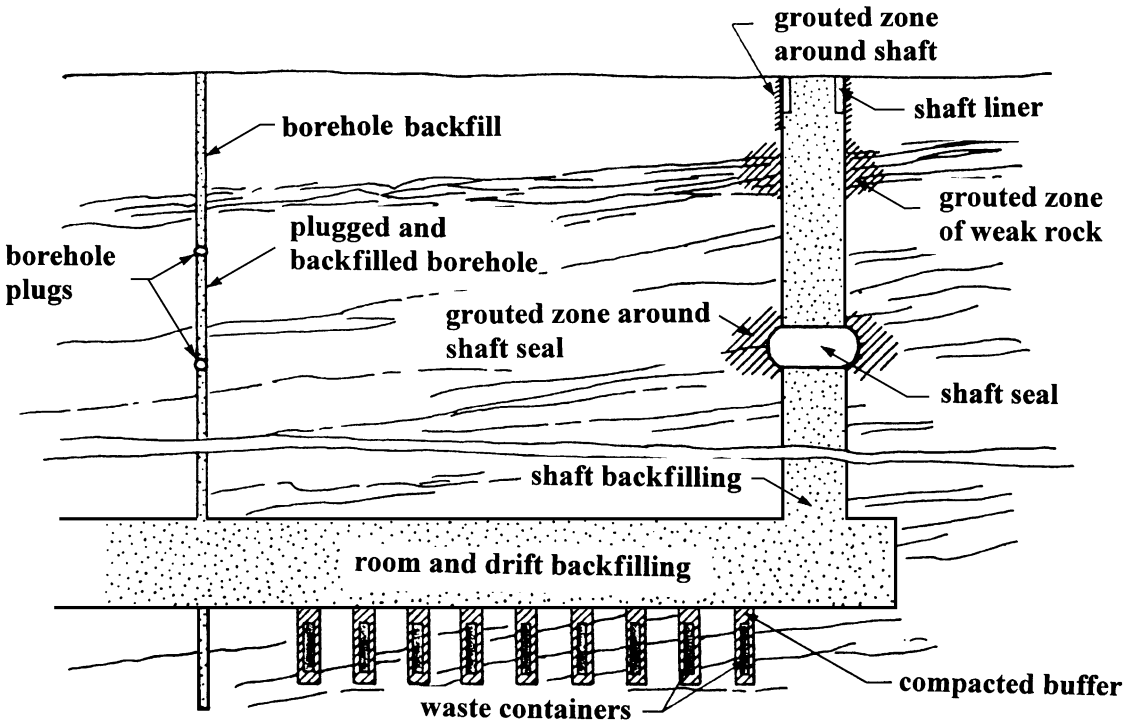

Fig. 1. Engineered barriers in a deep rock repository.

should be chosen in such a way that the conflicting constraints relating to heat conduction, swelling, radionuclide migration, strength, creep, etc., can be satisfied simultaneously. In the Canadian context, investigations conducted on the candidate buffer material for the determination of the heat conduction, moisture transport, radionuclide migration, creep and other mechanical interactions in the clay–sand buffer mixtures are discussed by Cheung and Chan (1983), Cheung et al. (1983), Radhakrishna (1984), Radhakrishna et al. (1990), Yong et al. (1985, 1986, 1990), Selvadurai (1992) and Selvadurai and Onofrei (1993). References to further works are also given by Gray (1993) and Selvadurai (1996a).

This paper discusses the experimental simulation of the heat-induced moisture movement in a bentonitic clay–crushed quartz–sand buffer, which is compacted within a borehole located in a granite block. The granite block contained an array of thermocouples that measured the temperature distributions along the planes of symmetry. The buffer material was compacted within the borehole in such a way that there was provision for the moisture influx at all the outer surfaces of the compacted buffer region. The granite block was hydraulically isolated through the provision of an impermeable membrane, which lined the borehole cavity. The internal heating was achieved by emplacing a cylindrical heater within the buffer during the compaction process. This paper summarizes the results of an experimental research program in terms of the documentation of the experimental results for the temperature distributions within the system and residual moisture distribution patterns within the buffer region when the buffer is internally heated at a constant power input and its outer boundary is subjected to the moisture influx at various levels of fluid pressure.

2. Experimental methodology and procedures

The Large Granite Block Test Facility used in the experimental research program is an instrumented granite block with cross-sectional dimensions of 918×926 mm and a height of 2446 mm. The granite block contains a cylindrical borehole approximately measuring 262 mm in diameter and 975 mm in depth. The granite block is instrumented with arrays of thermocouples that measure the temperature distributions along the orthogonal central planes of symmetry. Further details of the placement of the instrumentation are given in the paper by Selvadurai (1996a). In previous experiments involving this test facility (Selvadurai and Onofrei, 1993; Selvadurai, 1996a), attention was primary directed to the evaluation of the performance of the buffer materials that were subjected to internal heating with the provision of either the moisture efflux to the granite block or moisture containment within the buffer region through the provision of an impermeable geosynthetic lining at the borehole surface. Some limited experiments were also performed to allow the moisture influx to the compacted buffer region through its outer boundary at virtually zero pressure. In such experiments, a geotextile (a porous synthetic fabric of finite thickness) liner was placed adjacent to the impermeable membrane prior to in situ compaction of the buffer material. Such experiments were considered important from the point of view of the scoping calculations applicable to the extreme near field water influx conditions at a repository. In order to complete the range of these hygro-thermal experiments, it is necessary to establish the behaviour of the buffer under the combined influences of the internal heating and water supply at moderately large pressures. The water pressures that can be encountered at a repository can be very large depending upon the depth of location of such a repository and the rate at which the ground water conditions are allowed to reestablish upon the completion of the repository. These pressures can reach a maximum of 10 MPa for a repository located at a depth of 1000 m. In the experimental results reported, only the moderate fluid pressures are considered.

2.1. The modified Granite Block Test Facility

The Granite Block Test Facility cannot be directly used to conduct tests involving very large pressures (10 MPa) envisaged at a typical repository location. First, the open surface of the borehole has to be adequately sealed to realize such high pressures. Past experience with the pressurization of the borehole emplacement configuration indicated that it was extremely difficult to achieve a reliable high-pressure seal directly between the surface of the granite block and cover plate. Furthermore, the direct application of

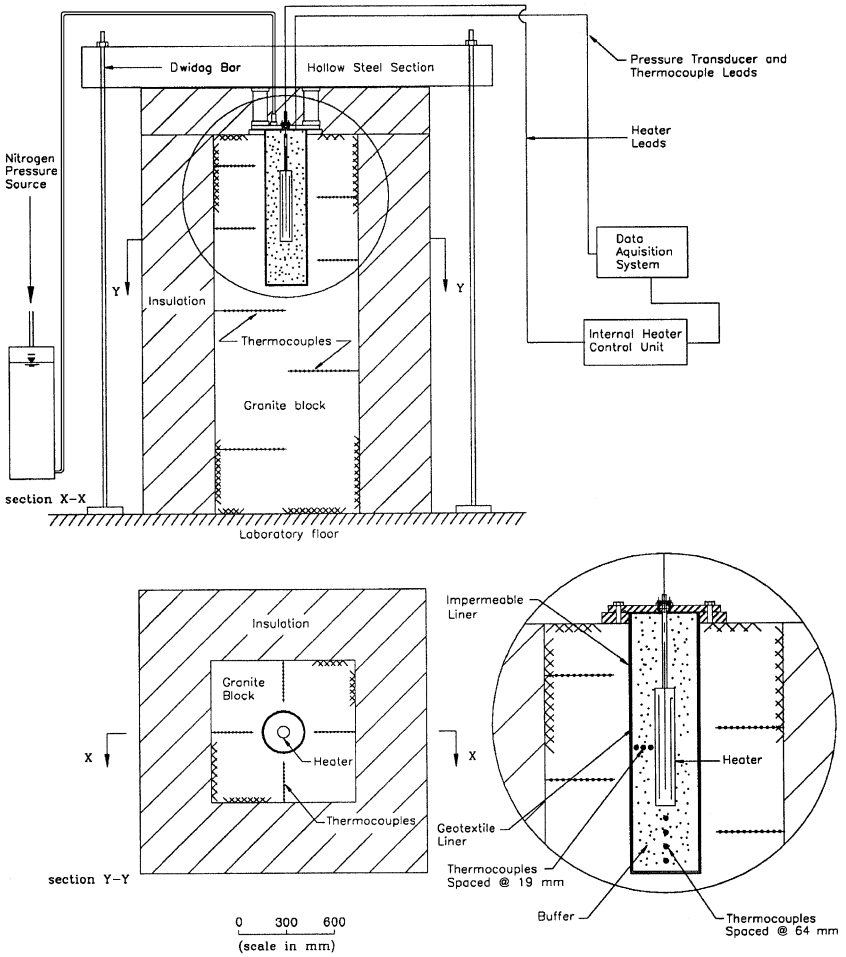

Fig. 2. The Granite Block Test Facility: modifications for the pressurized water influx at the buffer boundary.

high pressures at the boundary of the borehole will induce high circumferential tensile stresses at the borehole surface. At operating pressures even in the order of 2 MPa, there is an insufficient factor of safety for the purposes of conducting laboratory tests with respect to the initiation of damage and fracture at the cylindrical borehole surface and in the vicinity of the base of the borehole.

In order to utilize the Granite Block Test Facility for testing at moderately high pressures (up to 1 MPa), the surface of the borehole region was incorporated with a steel plate with a thickness of 37.5 mm. The steel plate was grouted to the surface of the granite. The junction between the steel plates was sealed with a cementing agent to provide a smooth transition. The cover plate for the borehole was a 25-mm thick stainless steel plate fitted with a Viton O-ring™ capable of withstanding high temperatures and pressures. The cover plate also contains a bearing seal that allows a hollow shaft, which is connected to the heater, to pass through it. The pressurized water is supplied to the boundary of the compacted buffer through the provision of a porous geotextile lining. Water migration to the rock is prevented by the geosynthetic liner (approximately 1 mm in thickness), which is placed adjacent to the borehole surface. The buffer is compacted within the geotextile lining (Figs. 3 and 4). The cover plate also contains two adaptors

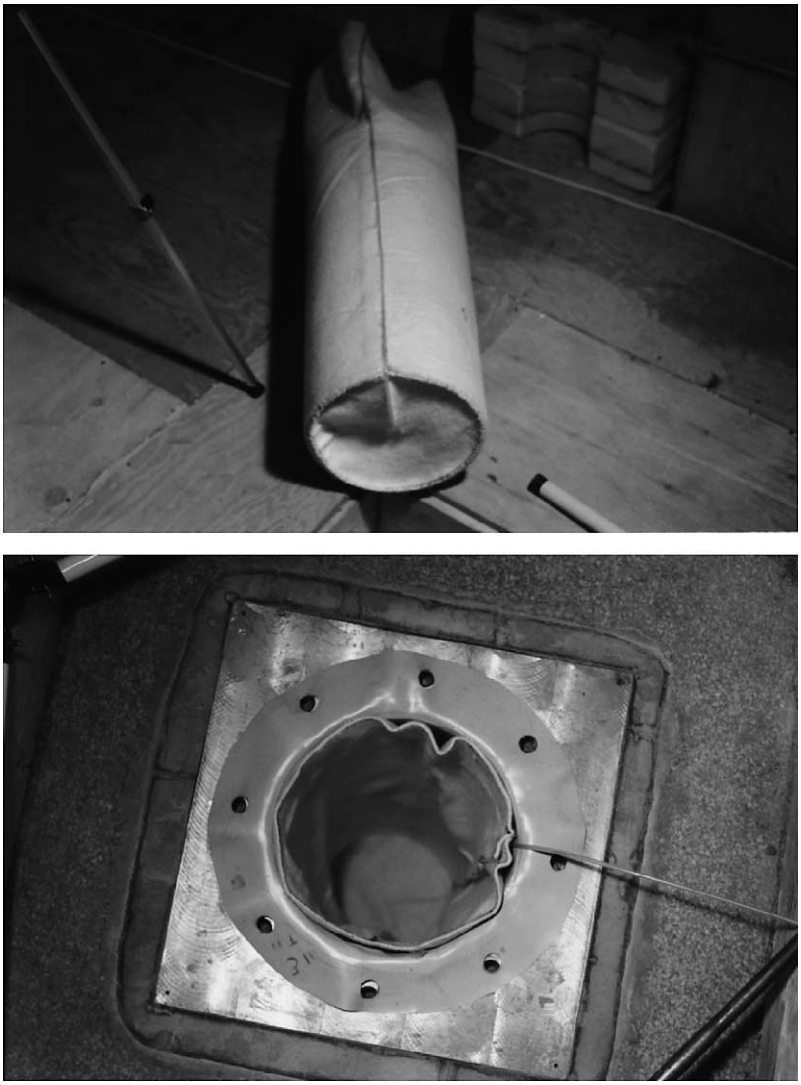

Fig. 3. Impermeable geosynthetic liner and geotextile porous interface.

that are pressure and temperature resistant. These couplings were used to guide the leads of the thermocouples that were used to measure the temperature at selected locations within the buffer region. These couplings are identical to those used in previous investigations (Selvadurai and Cheung, 1991; Selvadurai, 1996a). In order to eliminate the possibility of moisture migration through the sheath of the thermocouple wires, the coverings were removed and the bare thermocouple wires were secured to the coupling using the cementing agent Devcon™. The cover plate also has inlet and outlet ports that allowed the water influx and aggress from the outer boundary of the buffer region. The general arrangement of the modified Granite Block Test Facility is shown in Fig. 2.

2.2. The cylindrical heater

The cylindrical heater had to be specially designed to accommodate the requirements of the high-pressure testing and for the provision of a nearly uniform temperature distributions along its length, to better

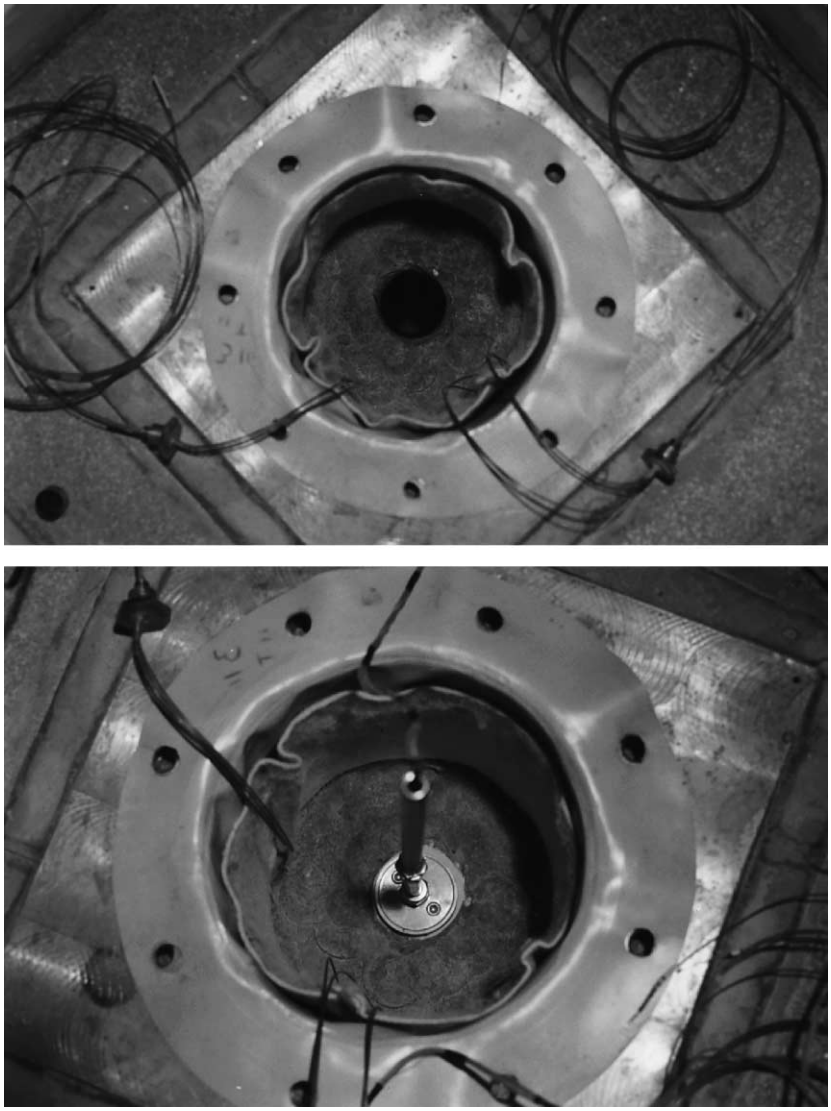

Fig. 4. Excavation of the compacted buffer and placement of the cylindrical heater.

simulate the thermal performance of a waste container. The heater consisted of a stainless steel (316 l) container shell of length 457 mm, diameter 73 mm and wall thickness 4.76 mm. The heating was provided by a Chromalox™ cartridge heater, which was positioned along the axis of the shell. The lower end of the heater contained a stainless steel plate where a Viton O-ring™ seal was incorporated. The upper end of the heater was also fitted with a stainless steel plate and a Viton O-ring™ seal. The upper plate also contained a Swagelok™ fitting to which a length of hollow PTFE tubing was attached. The heater cartridge was positioned by fitting the stainless steel discs at the upper and lower ends. The gap between the stainless steel cylinder and the heater element was filled with fiberglass insulation. The heater was also incorporated with six Type-K thermocouples to measure the temperature at the inner surface of the heater shell and at the upper, midsection and base levels of the heater. The thermocouple leads were routed

through the hollow PTFE tubing and through the case hardened hollow shaft. This procedure ensured that the heater coils would not interact with water under a high pressure. The hollow shaft also allows the heater to be externally vented, thereby eliminating the internal pressure buildup during the heating phase of the experiment. The general internal arrangement of the heater is shown in Fig. 5. Preliminary tests were performed on the heater in an ambient environment to establish the distribution of temperature along its length. These tests indicated that the temperatures at the ends of the heater were higher than those at the central plane. The arrangement of the stainless steel discs at both ends was altered (mostly by trial and error) so that a near uniform distribution of temperature was obtained under the ambient heating the heater, under the partial insulation and at a constant power supply.

The heater was initially placed within the borehole lined with a specially fabricated geosynthetic liner. The lined borehole cavity was filled with water and the entire system pressurized to about 1 MPa for a period of 24 h. The pressurized water was supplied via a water/pressurized nitrogen supply. The procedure was repeated in order to ensure that the seals performed in a reliable manner. These pressure tests did not incorporate any heating of the system. All seals used both in the fabrication of the heater and in the

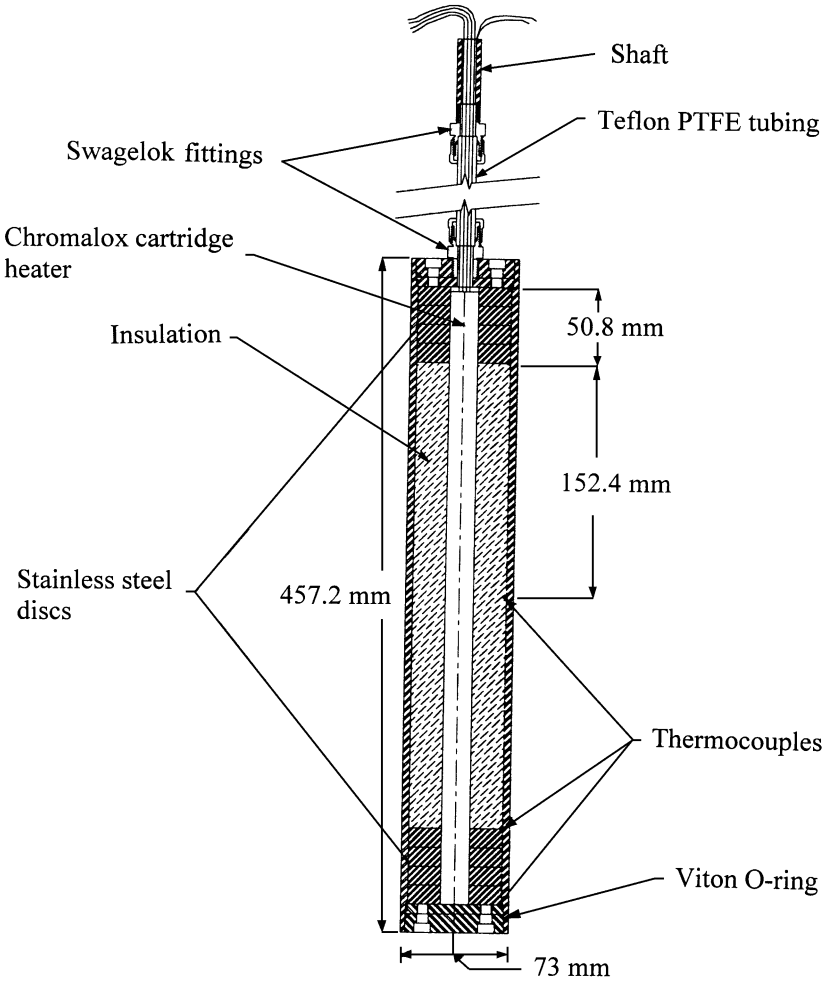

Fig. 5. Details of the cylindrical heater.

sealing of the borehole were supplied by the manufacturer to perform with reliability over the temperature and pressure range of interest to these experiments. The reaction frame used to load the borehole cover plate and to activate the O-ring seal incorporated in the plate consisted of a hollow steel section that was anchored to the laboratory's strong floor (Fig. 2).

2.3. The compaction and instrumentation of the buffer material

The buffer mixture, containing equal parts by weight of bentonitic clay and crushed quartz sand, had an average initial gravimetric moisture content $m = 17.8\%$ (average specific gravity of the soil particles $G_s = 2.70$). The impermeable geosynthetic bore-

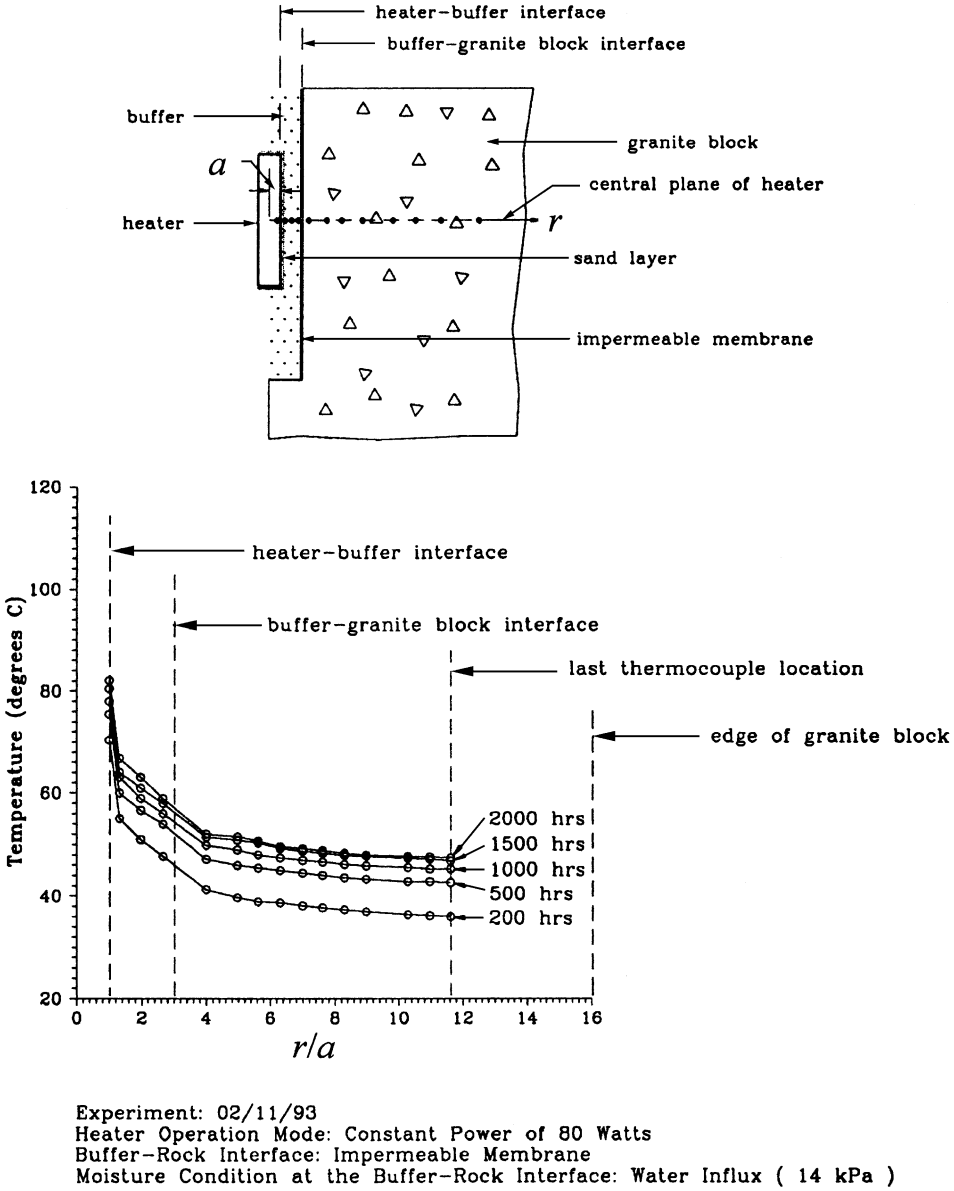

Fig. 6. Distribution of temperatures at the midsection plane of the heater (water influx pressure = 14 kPa).

hole liner was first placed in the borehole and a permeable geotextile lining was then placed immediately adjacent to it. A polyethylene tube with an approximate diameter of 3 mm was attached to the geotextile lining. The end of this tube was located at the flat base of the geotextile lining and enabled the moisture supply at the boundary of the buffer during the experiments. The geotextile lining and geosynthetic liner were first compressed against the borehole using a plastic former. Compaction of the buffer material was carried out in lifts (approximately 2060 g) using the modified Proctor hammer. Altogether, 125 blows of the hammer were used to compact each layer; a total of 45 compaction lifts were required to

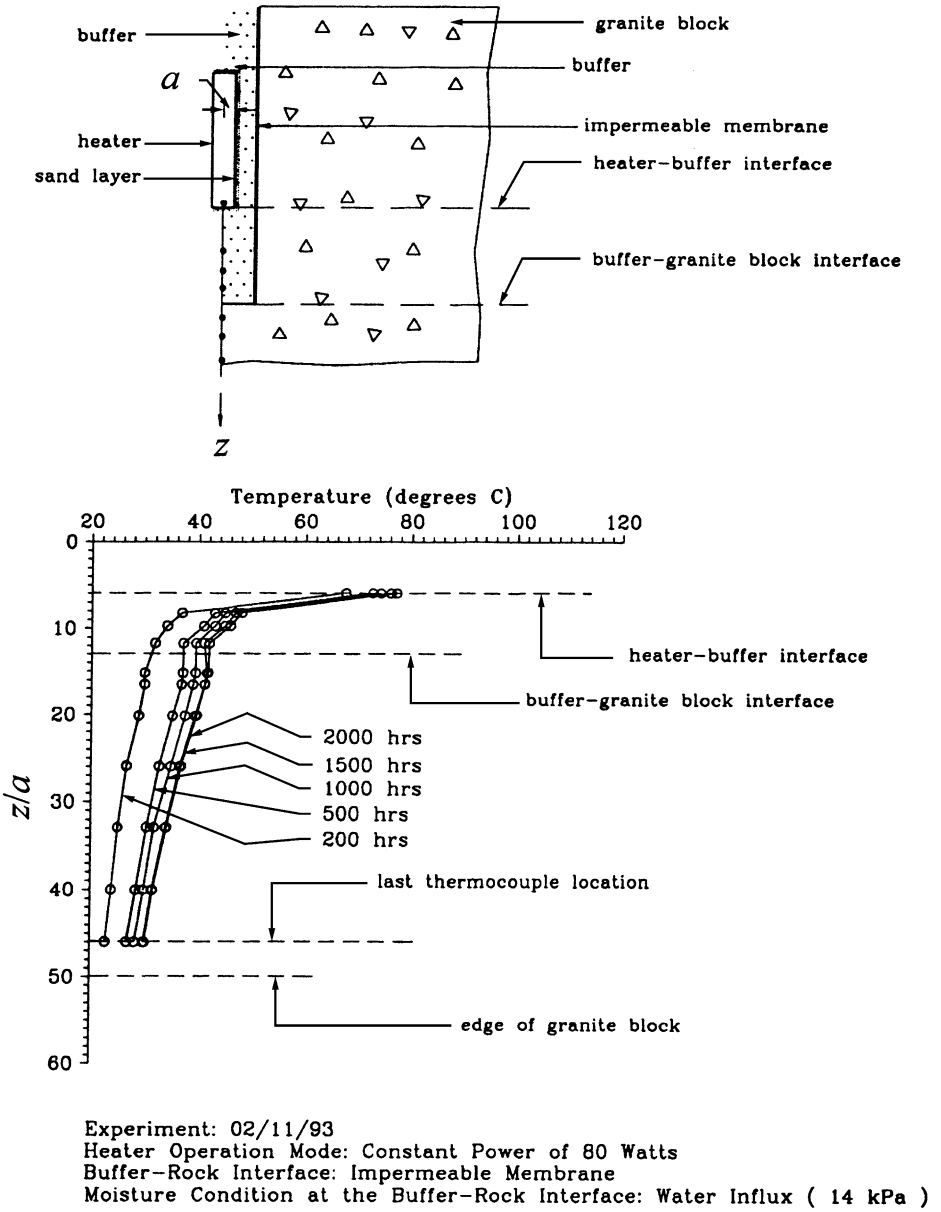

Fig. 7. Distribution of temperatures along the axis of the buffer and the granite block (water influx pressure = 14 kPa).

fill the borehole cavity. The approximate bulk unit weight of the buffer in its compacted state was $\gamma = 19.5$ kN/m^3 and the dry unit weight $\gamma_d = 16.6$ kN/m^3. The initial void ratio of the compacted buffer was estimated at $e_0 = 0.63$. The initial degree of saturation was $S_0 = 76\%$ and the initial volumetric moisture content, $\theta_0 = 29\%$. The volumetric water content θ is related to the gravimetric water content m and the degree of saturation S through the relationships

$$\theta = \frac{m\gamma_d}{\gamma_w} = \frac{Se}{(1+e)} \quad (1)$$

where γ_w is the unit weight of water. Since most of the work associated with the moisture movement in the unsaturated media refers to the representations in terms of the volumetric moisture content θ, we shall use this measure to represent the moisture distributions in the compacted buffer during the moisture influx process. In the experiment where the water influx was at a nominal pressure of 14 kPa, a total of seven thermocouples were installed within the buffer material during its compaction; three thermocouples were placed radially, approximately 18 mm apart in a plane that roughly corresponded to the midsection level of the heater; and four thermocouples were located along the axis below the base of the heater and at an interval of 62.5 mm (the axially positioned thermocouple closest to the heater was damaged during the installation of the heater). In the

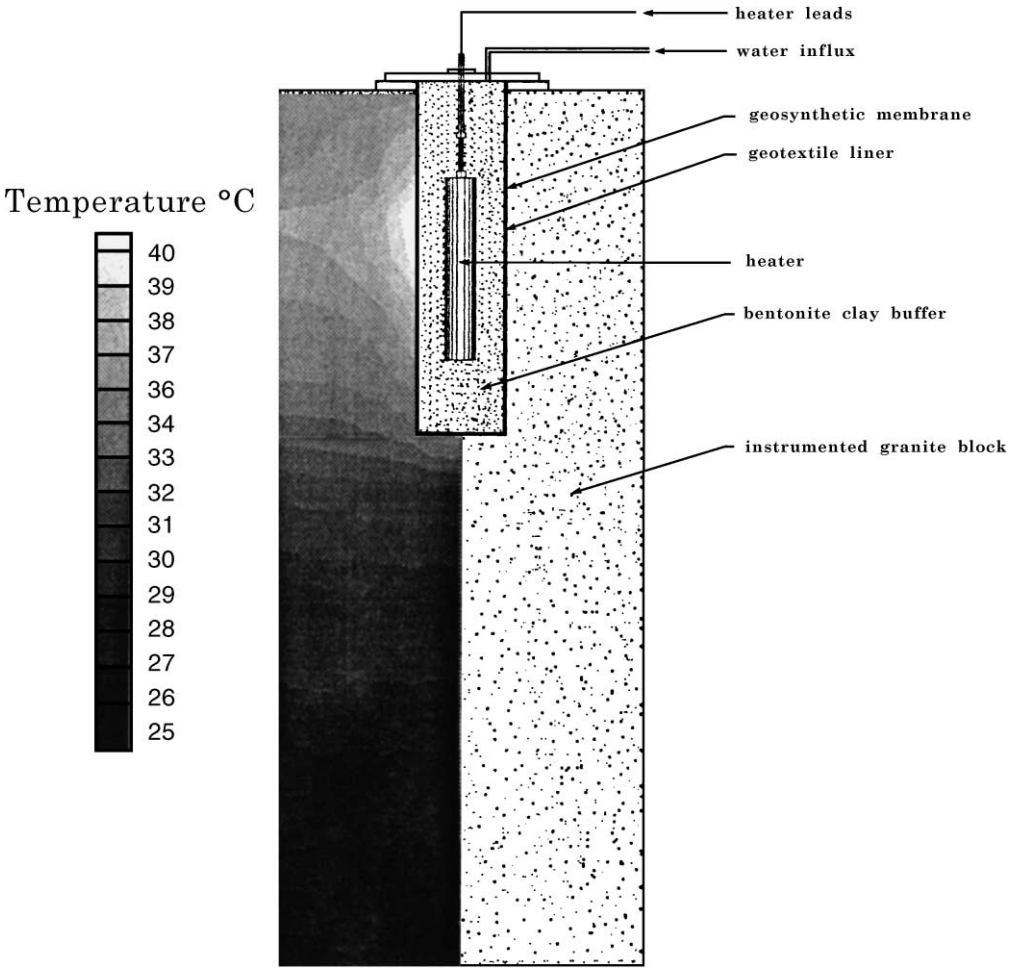

Fig. 8. Temperature contours within the granite block at 200 h (water influx pressure = 14 kPa).

experiments where the water influx was at 345 and 420 kPa, no thermocouples were incorporated within the buffer. This was intended to minimize the possible pathways for the localized moisture migration (along the boundary of the thermocouple leads) during the pressurization of the outer boundary of the compacted buffer.

2.4. Installation of the heater and preparation for testing

The buffer was first compacted to the specified upper level of the heater. The cavity in the compacted buffer for the placement of the heater was formed using a wood drill bit with a diameter of approximately 77 mm. The base of the cavity was leveled and a layer of fine sand about 3 mm thick was placed to receive the heater. The approximately 5-mm gap between the heater and the buffer cavity was filled with uniformly graded fine sand with a maximum particle size of 0.5 mm. Further details of the heater installation procedure adopted in previous experiments are given by Selvadurai (1996a) and a general view of the heater placement in the current series of experiments is also shown in Fig. 4. The remainder of the buffer material, above the upper level of the heater, was compacted, ensuring that the Teflon™ tubing and hollow shaft were maintained in a nearly axial position. The flexibility of the

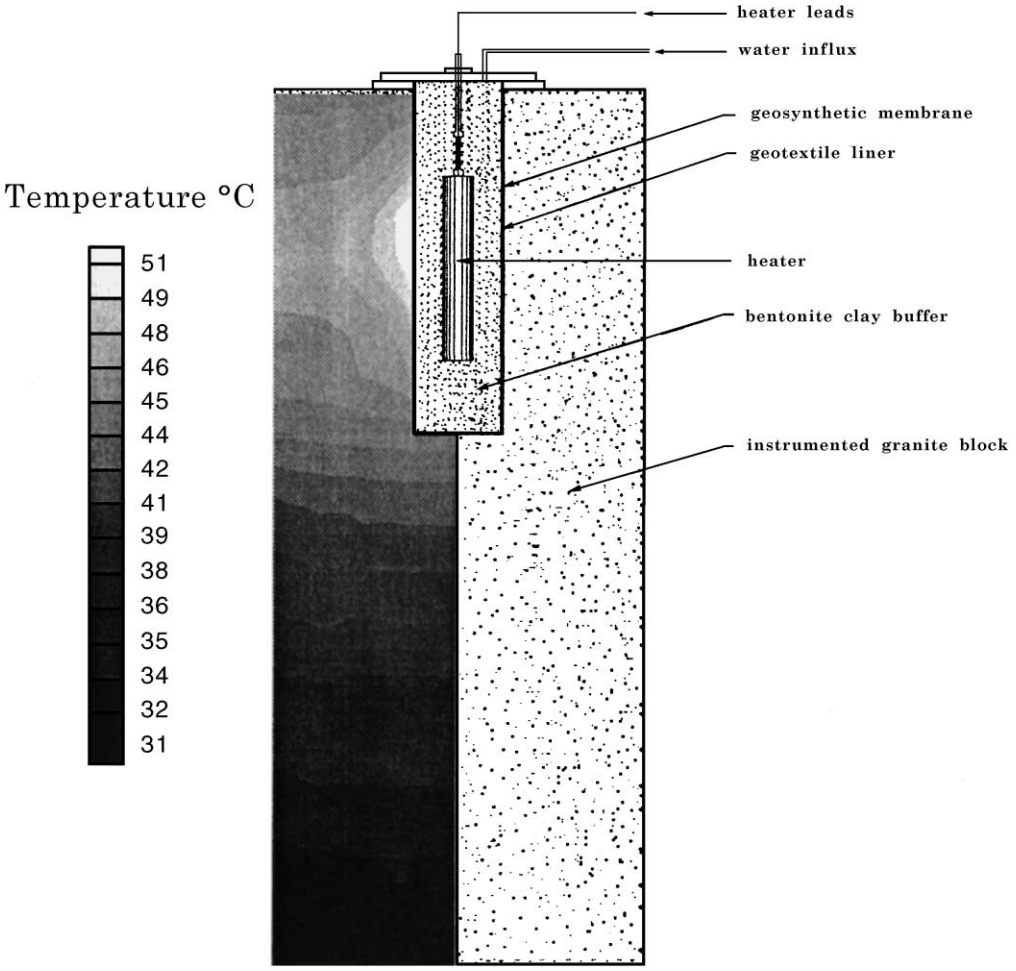

Fig. 9. Temperature contours within the granite block at 2000 h (water influx pressure = 14 kPa).

Teflon™ tubing allowed this alignment process without damage to the fittings and pressure seals. Upon the completion of the compaction process, a circular pad of geotextile material was placed at the upper surface of the buffer. The cover plate was attached to the steel plate at the surface of the granite block. Finally, after the completion of the connections to the heater leads, thermocouple leads, water influx connections, etc., the cover plate was anchored to the laboratory floor with the aid of an anchoring system to ensure the complete sealing of the emplacement borehole (Fig. 2).

3. Experimental results

Three experiments involving the pressurized water influx at the buffer–rock interface were conducted using the modified Granite Block Test Facility. The first experiment dealt with the water influx to the compacted buffer at a nominal pressure of 14 kPa. The heater was supplied with a constant measured power input of 80 W. Fig. 6 illustrates the distribution of temperature at the mid-plane level of the heater at lapsed times of 200, 500, 1000, 1500 and 2000 h. The positions of the thermocouples are normalized with respect to a, the radius of the heater. Temperature readings from the thermocouples, located both within the buffer region and within the granite block, are used in these graphical representations. Similarly, Fig. 7 shows the distribution of temperature along the axis of the heater at lapsed times of 200, 500, 1000, 1500 and 2000 h.

The positions of the thermocouples within the granite block are different on the two planes of vertical symmetry about the axis of the borehole. These thermocouple data, however, can be grouped to generate an idealized composite thermographic representation within one plane of symmetry. In such a data processing exercise, it is also convenient to further assume that the temperatures are symmetric about an axis of symmetry. The time histories of the temperature at discrete points are used in conjunction with a spatial interpolation technique (available through commercially available software) to generate the thermographic displays of the heat conduction within the granite block. Figs. 8 and 9 illustrate the thermographic displays of the temperature distributions within the granite block at 200 and 2000 h, obtained for the experiment where the boundary of the compacted buffer was subjected to the water influx at a nominal pressure of 14 kPa.

An inspection of the temperature distributions shown in Figs. 6 and 7 indicates that the surface temperatures at the midsection level of the heater and at the base of the heater roughly correspond to 82 and 77 °C, respectively. The internal configuration of the heater consequently gives a relatively uniform surface temperature distribution in the embedded condition. The heater test was terminated at 2000 h and the system was allowed to cool for a period of 48 h. The moisture sampling was carried out immediately there-

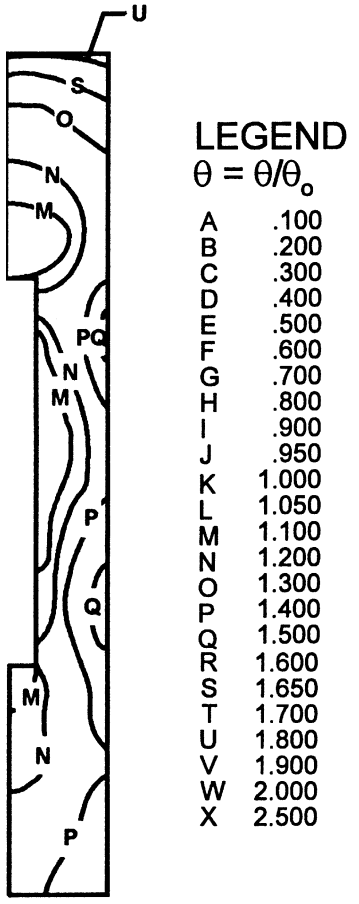

Fig. 10. Distribution of residual volumetric moisture content in the buffer (temperatures are normalized with respect to the original volumetric moisture content, test conducted at a water influx pressure = 14 kPa).

after. The sampling involved coring to a specified depth and retrieving the samples from the base of the borehole. Three 75-mm diameter boreholes were drilled in the buffer at 120° apart and five samples were obtained from each borehole at each level. Altogether, 300 samples were retrieved from the buffer region at 20 levels. The remaining 84 samples relate to the boreholes, which were drilled along the axis of the buffer both above and below the heater. The contours of the residual volumetric moisture content $\theta(\bar{r},\bar{z})$ (where r is measured from the axis of the heater, z is measured from the base of the heater, $\bar{r}=r/a$, $\bar{z}=z/a$ and a is the radius of the heater), shown in Fig. 10, represent the volumetric moisture content θ

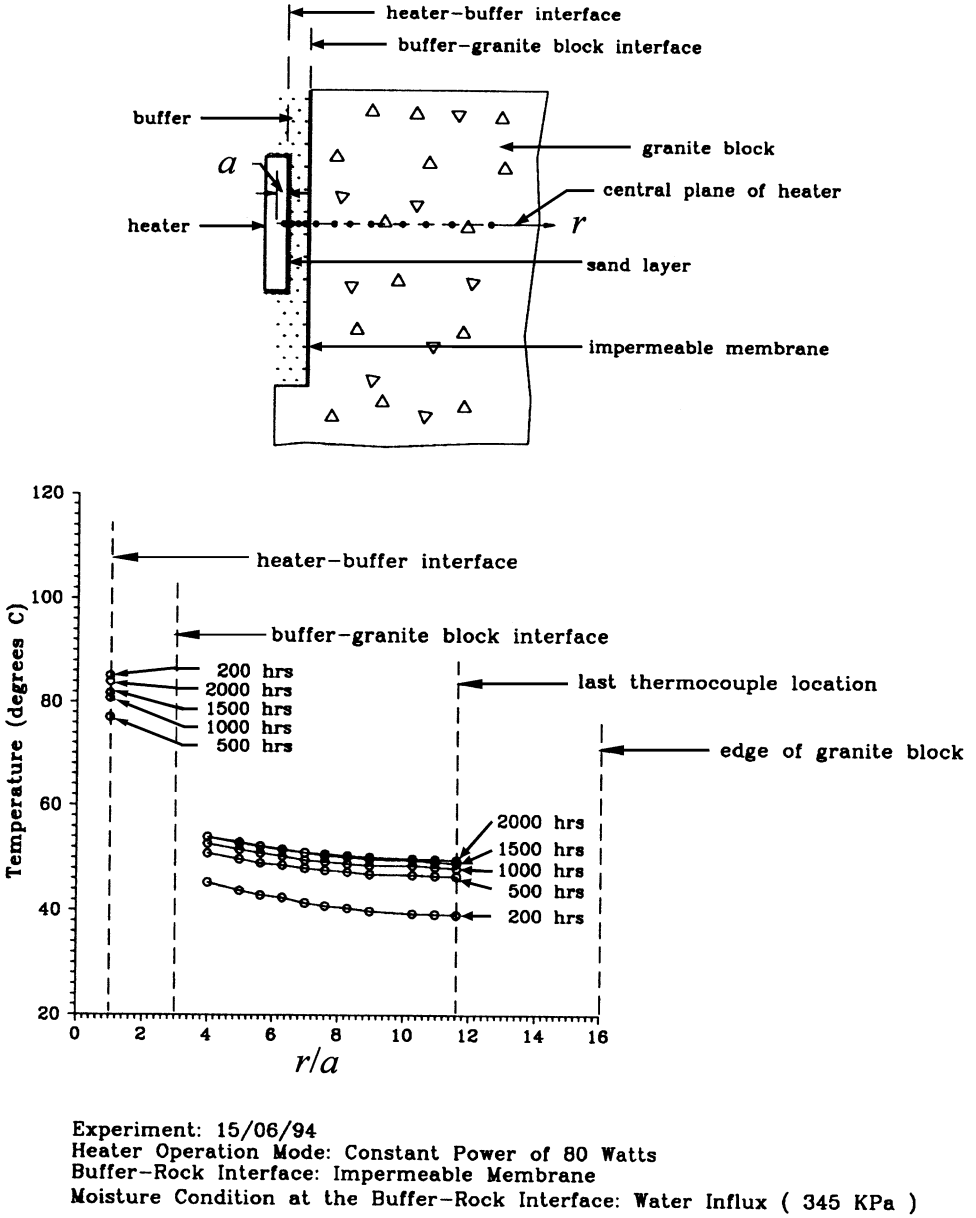

Fig. 11. Distribution of temperatures in the granite at the midsection plane of the heater (water influx pressure = 345 kPa).

normalized with respect to the initial volumetric moisture content $\theta_0 = 29\%$. The total volumetric moisture content is obtained approximately by considering the discretization of the buffer region into the annular elements in the radial direction. The height of the annular elements is kept equal to the difference in radii of the annular elements. These results also compare favourably with the alternative calculation involving the average volumetric moisture content distribution over the cross-section of the buffer region, the location of the center of area of the weighted average of the volumetric moisture content about the axis of the buffer and the longitudinal cross-sectional area of the buffer region (this involves the application

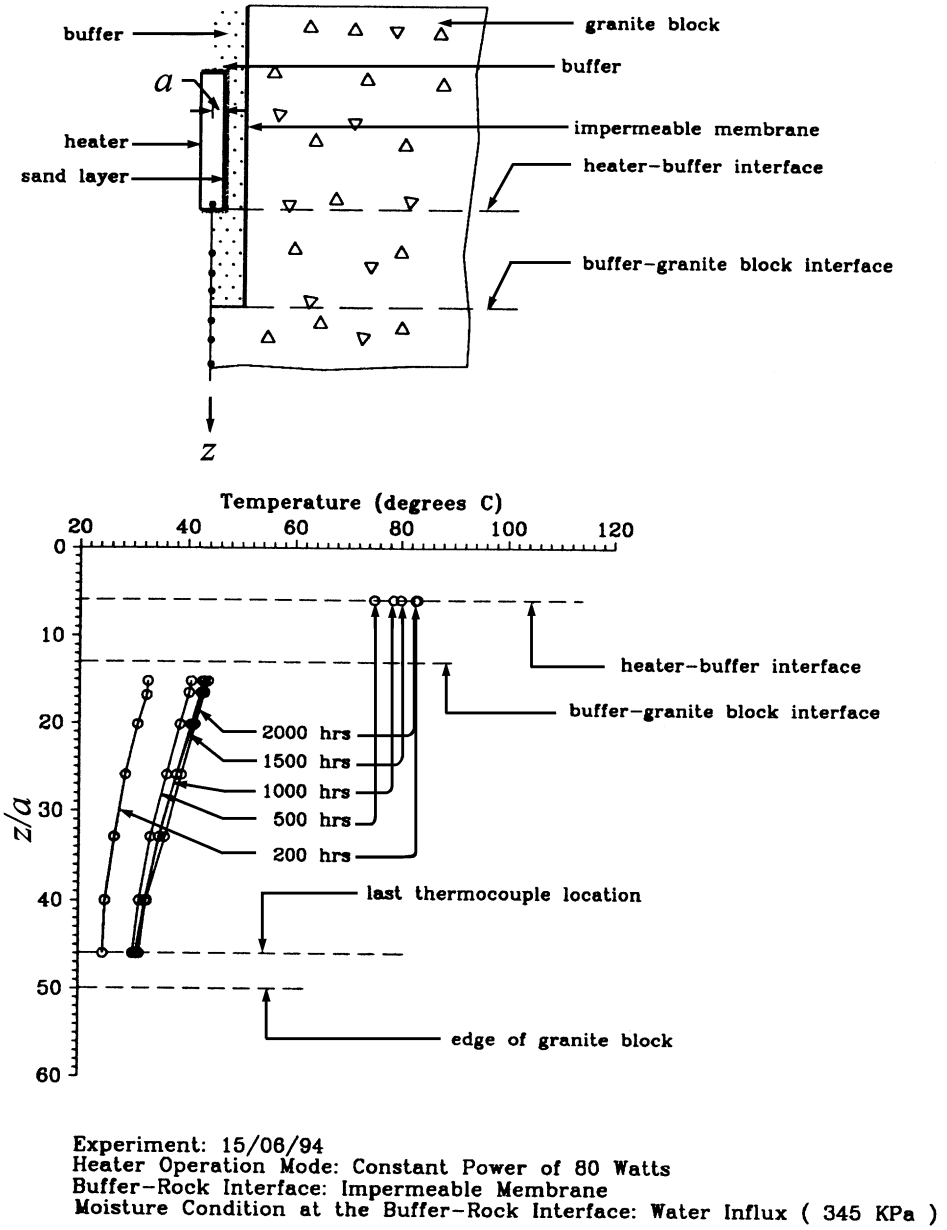

Fig. 12. Distribution of temperatures along the axis of the granite block (water influx pressure = 345 kPa).

of a modified form of the 'Theorem of Pappus'). The net moisture absorption within the buffer region can be estimated from either the gravimetric moisture content or volumetric moisture content determined at the termination of the test. It was found that at near termination of the experiment at $t = 2000$ h, the average volumetric moisture content within the buffer region had increased to $[\theta_{ave}]_{14\ kPa} \cong 34.9\%$, due to the moisture absorption from the boundary of the buffer. The resulting average degree of saturation of the buffer approximately corresponds to 91%.

In the second test, the heater was operated at a constant power input of 80 W and the boundary of the buffer region was maintained at a water pressure of 345 kPa. Fig. 11 illustrates the distribution of the temperature at the mid-plane level of the heater at a time duration of 200, 500, 1000, 1500 and 2000 h. Fig. 12 gives the equivalent data for the temperatures along the axis of the test facility. The temperature distributions within the granite block were also used to generate the thermographic displays, Figs. 13 and 14 illustrate the thermographic displays of temperature within the granite block obtained at 200 and 2000 h, respectively. The moderately high-pressure (345 kPa) heater test was terminated at 2000 h and the system was allowed to cool down for a period of 48 h. The moisture sampling was carried out using the procedures identical to those described previously. Fig. 15 illustrates the contours of the residual values of the normalized volumetric moisture content within the

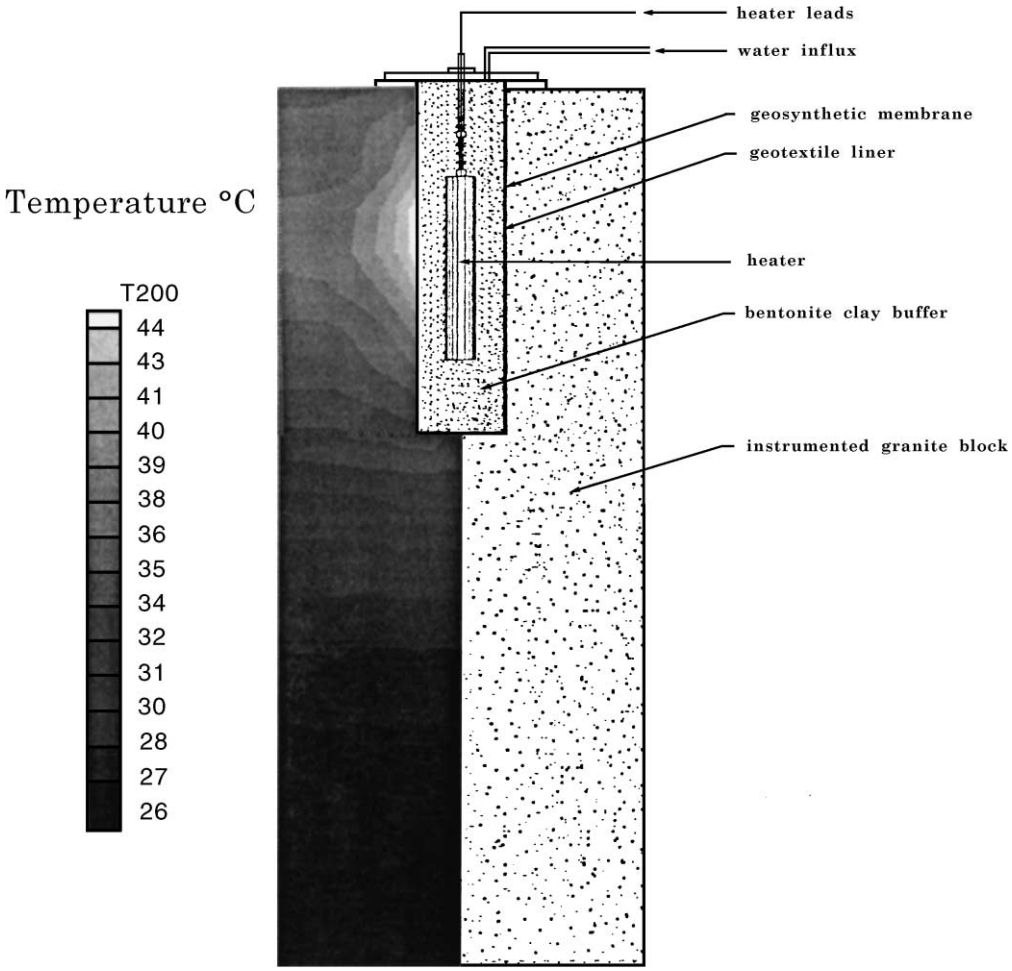

Fig. 13. Temperature contours within the granite block at 200 h (water influx pressure = 345 kPa).

buffer region at near termination of the experiment. It was found that, at the termination of the experiment, the average volumetric moisture content within the buffer region had increased to $[\theta_{ave}]_{345\ kPa} \cong 36.5\%$, due to the moisture absorption from the boundary of the buffer. The resulting degree of saturation of the buffer region approximately corresponds to 95.3%.

In the third experiment, the boundary of the buffer region was maintained fully saturated at a water pressure of 420 kPa. The heater was operated at a constant power input of 80 W. The distributions of temperature within the granite block at the midsection level of the heater and along the axes of symmetry were very similar in both the magnitude and spatial variation to the temperature distributions derived from the previous experiments (see Figs. 11 and 12) where the exterior surface of the buffer was maintained at a water pressure of 345 kPa, consequently; they are omitted to conserve space. Fig. 16 illustrates the contours of the normalized residual volumetric moisture content within the buffer after a 48-h period following the termination of the test. In this experiment, it was found that the average volumetric moisture content within the buffer region had increased to $[\theta_{ave}]_{420\ kPa} \approx 43\%$. The corresponding average degree of saturation within the buffer region consistent with the initial void ratio of 0.63 would amount to 112%. Clearly, this result implies that there is an expansion in the soil skeleton to accommodate this increase. Assuming the average degree of saturation is

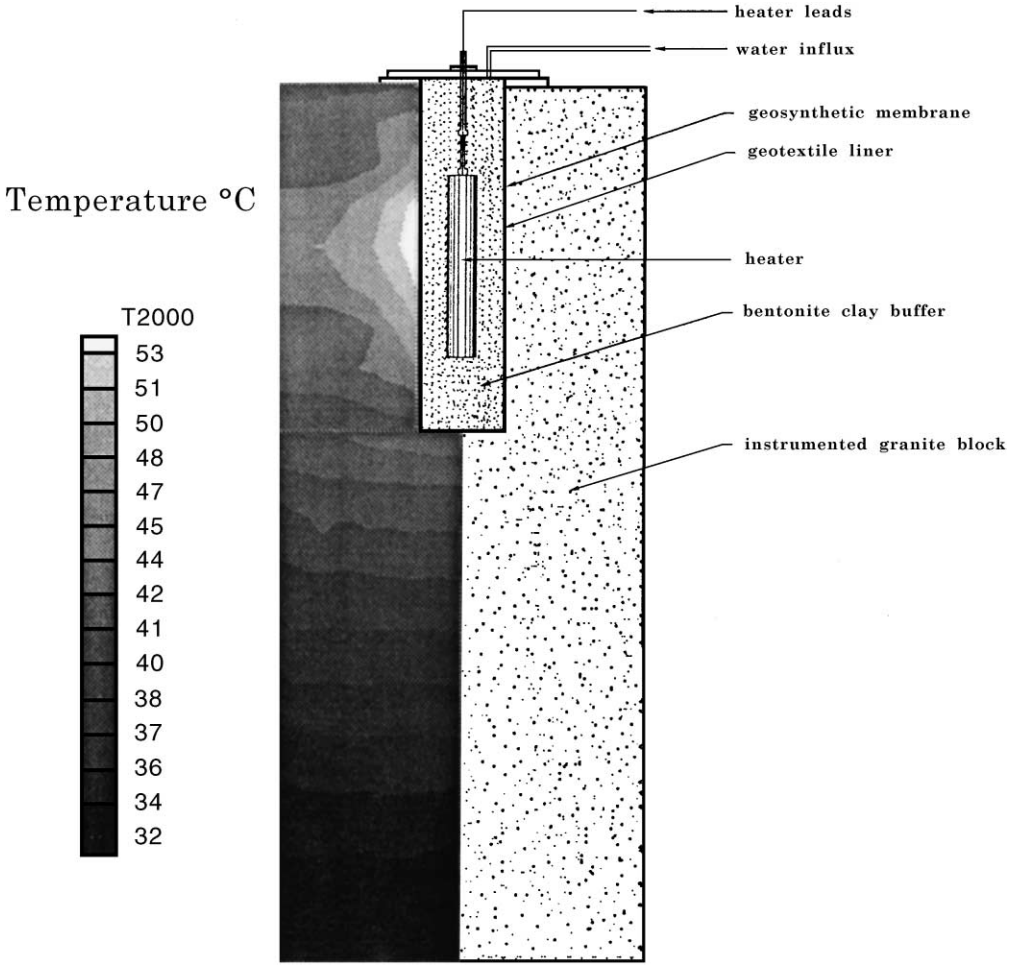

Fig. 14. Temperature contours within the granite block at 2000 h (water influx pressure = 345 kPa).

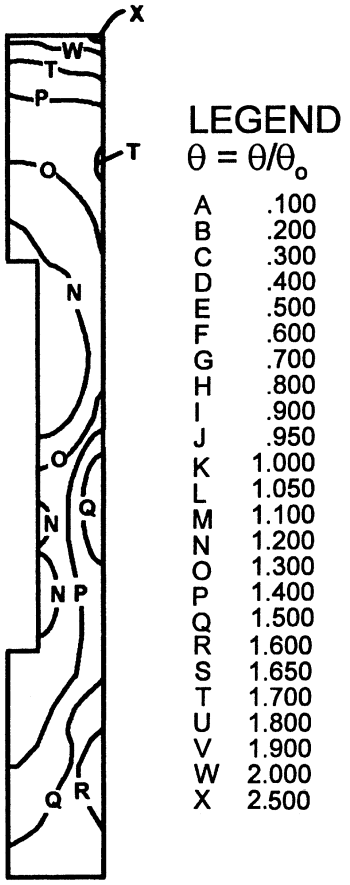

Fig. 15. Distribution of residual volumetric moisture content in the buffer (volumetric moisture contents are normalized with respect to the original volumetric moisture content, test conducted at a water influx pressure = 345 kPa).

100%, the corresponding average void ratio would now increase to 0.76. Considering the phase relationships, it can be shown that

$$\frac{V_f}{V_i} = \frac{(1 + e_f)}{(1 + e_i)} \tag{2}$$

where the suffix 'i' corresponds to the initial state, the suffix 'f' corresponds to the final state in a porous medium where the void ratio changes with the constancy of the solid contents, and V refers to the total volume. A volumetric strain ε_v can be defined as

$$\varepsilon_v = \frac{V_f - V_i}{V_i} = \frac{(e_f - e_i)}{(1 + e_i)}. \tag{3}$$

Considering the initial void ratio at the compaction of the buffer ($e_i = 0.63$) and the average void ratio corresponding to the complete saturation ($e_f = 0.76$), the result (Eq. (3)) gives a volumetric expansion of approximately 8.64% or a corresponding linear expansion of approximately 2.88%. Considering the radial dimensions of the buffer, this would approximately translate to a 7-mm expansion of the 262-mm section and an approximately 2.7-mm expansion of the annulus of the material dimension of 93 mm. Although the buffer is compacted in situ, the swelling pressure generated in the bentonite–sand mixture could conceivably result in the penetration of the outer regions of the softened saturated buffer into the geotextile material, which could accommodate the

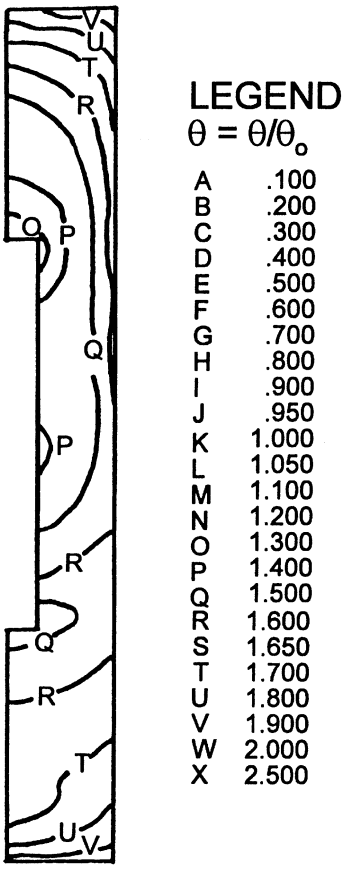

Fig. 16. Distribution of residual volumetric moisture content in the buffer (volumetric moisture contents are normalized with respect to the original volumetric moisture content, test conducted at a water influx pressure = 420 kPa).

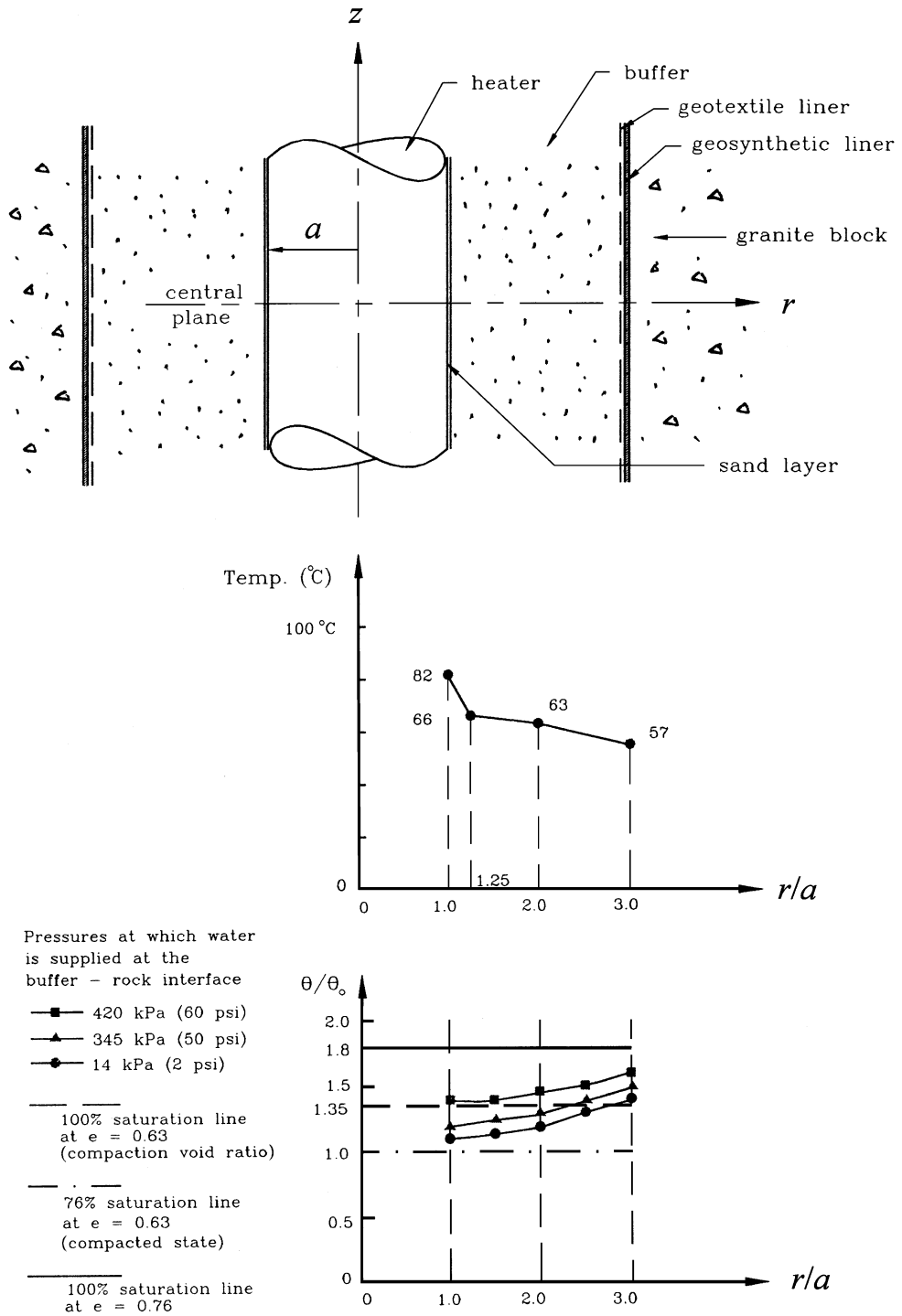

Fig. 17. Distribution of the volumetric moisture content within the buffer at the mid-plane section of the heater.

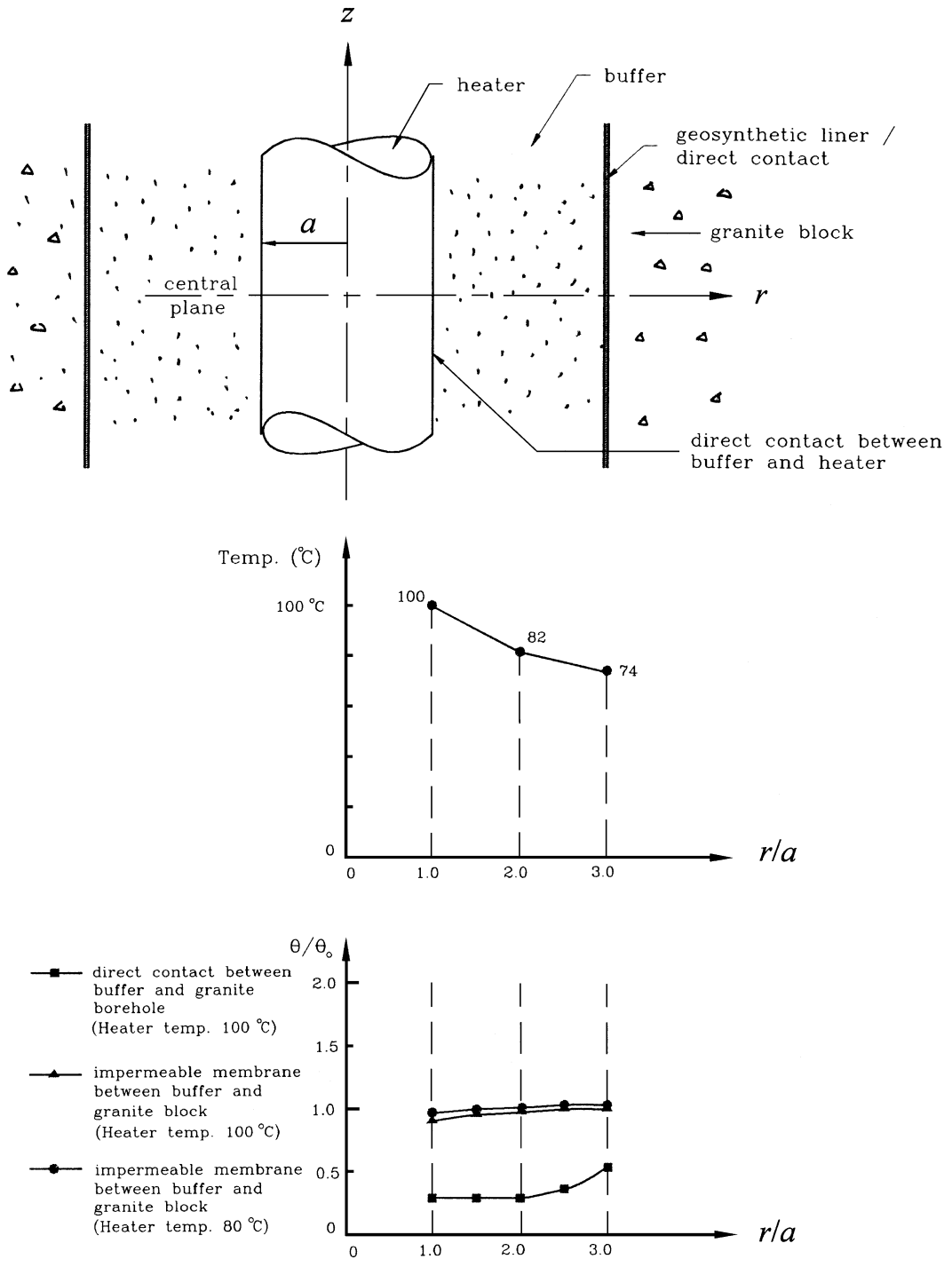

Fig. 18. Distribution of the volumetric moisture content within the buffer at the mid-plane section of the heater.

additional increase in the void ratio and the resulting changes in the dimensions of the buffer. This is a conjectural argument which can only be verified by studies which involve the measurement of changes in the buffer dimensions during the moisture uptake. Such experimentation is certainly non-routine and requires complicated non-invasive techniques for the measurement of both the moisture movements and deformations of the buffer during the moisture uptake and heating.

It is also convenient to provide a graphical representation of the moisture distribution patterns at the mid-plane level of the heater. Fig. 17 presents the variations in the residual values of the normalized volumetric moisture content corresponding to the three experiments where the moisture influx to the compacted buffer region takes place at different levels of the boundary fluid pressure. The saturation lines corresponding to the different values of the void ratios are also shown for reference purposes. In a previous series of experiments, tests were conducted where the buffer region was either in direct contact with the granite rock or was isolated by the provision of a geomembrane at the buffer–rock interface. There was no provision for the moisture influx at the boundary of the buffer. These experiments, however, were conducted with heater temperatures of 100 °C. Fig. 18 presents, for comparison purposes, the variations of the residual values of the normalized volumetric moisture content distributions, at the mid-plane level of the heater, for the tests in which either the compacted buffer was in direct contact with the granite or where the buffer–rock interface was provided with an impermeable membrane.

4. Concluding remarks

A large scale Granite Block Test Facility was used to conduct the laboratory experiments where the interface between the granite block and the compacted bentonitic clay–sand buffer was subjected to the combined action of water supply under pressure at the outer boundary of the buffer and internal heating. These experiments necessitated the development of the experimental procedures, which could accommodate pressures up to 1 MPa. In particular, the cylindrical heater used in the experiments was designed to achieve a near uniform temperature profile along its length. At a constant power supply of 80 W, the skin temperatures on the heater exhibited an axial differential value of approximately 5 °C. Although these temperatures were observed only at discrete locations, supplementary tests indicate the presence of a near uniform temperature along the surface of the heater. This aspect of the experimentation becomes important if any computational modelling (e.g. see Selvadurai, 1996b) of the hygro-thermal experiment is contemplated at a future date. In the experiments conducted, a geosynthetic liner was used in the borehole to act as a seal to prevent water migration to the dry granite block. The buffer was compacted within a geotextile lining, which supplied water to the outer boundary of the buffer at a specified pressure.

At the termination of the experiment with the water supply at 14 kPa, the average value of the volumetric moisture content θ_{ave} within the buffer region increased from its initial placement value of approximately 29%–34.9% during a 2000-h experiment. With this water absorption, and assuming that the void ratio remains constant at 0.63, this represents an average degree of saturation within the buffer of 90%. During the pressurized water supply to the boundary of the compacted buffer at 345 kPa, the average volumetric moisture content within the buffer region increased to 36.5%, or 95% saturation at the end of a 2000-h experiment. In the experiment where the moisture was supplied to the boundary of the compacted buffer at 420 kPa, the average volumetric moisture content within the buffer region increased to 43% or 112% saturation. In estimating these degrees of saturation, it is implicitly assumed that there is no alteration in the void ratio within the compacted buffer. It is evident from the results of the third test that there was a net increase in the void ratio of the buffer region as a result of the swelling activity at the outer boundary of the compacted buffer and the possible shrinkage in regions very close to the heater. The moisture sampling, however, indicates that there are only increases in the volumetric moisture content distributions throughout the buffer region in both experiments. Nevertheless, the relative changes in the void ratio can be dependent upon the relative increases in the volumetric moisture content within the buffer region. The results for the residual moisture distribution patterns obtained for the case where the buffer is in direct contact with the

granite indicate the severity of the moisture loss from the buffer to the granite during the heating and restricted moisture influx to the boundary of the buffer.

The temperature distributions within the buffer indicate the characteristic trends observed in previous heater experiments that were conducted in the absence of the moisture influx at the boundary of the buffer. There are sharp temperature gradients at the buffer–heater interface and these gradients are observed both at the midsection level of the heater and along the axis. The temperature distributions beyond the buffer–heater interface exhibit continuous time-dependent variations. This variation is evident in the experiment involving the water influx at low pressure. The trends in the temperatures observed within the granite block during the high-pressure water influx seem to suggest that, for the prescribed power input, the heat conduction process is in no way impeded by any drying action within the buffer. Also, with the experiment involving the direct contact between the buffer and the granite block, although there is a substantial loss of moisture from the buffer region, such losses do not diminish the ability of the buffer to maintain its heat conduction characteristics. It could be concluded that the efficient heat conduction characteristics of the buffer could be retained in instances involving both the internal heating and either the moisture influx or moisture loss at the outer boundary of the buffer. Such moisture retention characteristics of the buffer region are essential to maintaining its physical characteristics, including the elimination of the heat-induced desiccation of the clay buffer that can lead to the adverse performance of the buffer, particularly in its ability to minimize the radionuclide migration by diffusive processes.

The re-saturation of the buffer material after a prolonged heating in the absence of the moisture influx is a point of concern in establishing the integrity of the buffer. Such a scenario is consistent with the initial stages in the operation of a repository. These preliminary results and those of a previous series of experimental investigations involving the Granite Block Test Facility seem to indicate that at the reference temperatures envisaged for the proposed disposal schemes for the heat emitting wastes (i.e. reference temperatures $< 100\ ^{\circ}C$), the buffer is capable of maintaining both its water absorption and heat conduction characteristics and that such processes can be enhanced by the ambient fluid pressure levels at the repository location. Whether the changes in the initial moisture depletion in the buffer during the restricted moisture supply and re-saturation results in the corresponding changes in the transport characteristics of radionuclides is an open question which merits further investigation.

Acknowledgements

The work described in this paper was supported in part by a Research Grant awarded by the Natural Sciences and Engineering Research Council of Canada and in part by a Research Contract issued by the Waste Management Branch of AECL, Pinawa, Man. The work was performed at the Civil Engineering Laboratories at Carleton University, Ottawa, Ontario, Canada. The author is grateful to Messrs. K. Trischuk, R. Weidelich, K.C. McMartin, and S.D. Conley for their assistance with the experimentation.

References

Chapman, N.A., McKinley, I.G., 1987. The Geological Disposal of Nuclear Waste Wiley, New York.

Cheung, S.C.H., 1990. A new interpretation of measured ionic diffusion coefficients in compacted bentonite-based materials. Eng. Geol. 28, 369–378.

Cheung, S.C.H., Chan, T., 1983. Computer simulation of contaminant transport. Proceedings of the Computer Simulation Conference, Vancouver, vol. 1, pp. 470–475.

Cheung, S.C.H., Oscarson, D.W., Lopez, R.S., 1983. Factors influencing mass diffusion in bentonite and mixtures of bentonite and sand. Scientific Basis for Nuclear Waste Management. Proc. Materials Research Society, vol. 26, pp. 711–718.

Design and instrumentation of in situ experiments in underground laboratories for radioactive waste disposal. In: Come, B., Johnston, P., Muller, A. (Eds.), 1985. Proceedings of Workshop, Jointly Organized by Commission of European Community and OECD Nuclear Waste Energy Agency, Brussels. A.A. Balkema, The Netherlands.

Fujita T. et al., 1997. Fundamental Properties of Bentonite OT-9607, Power Reactor and Nuclear Fuel Development Corporation Report, PNC TN 97-071.

Gens, A., Garcia-Molina, A.J., Olivella, S., Alonso, E.E., Huertas, F., 1998. Analysis of a full scale in situ test simulating repository conditions. Int. J. Numer. Anal. Methods Geomech. 22, 515–548.

Gnirk, P., 1993. OECD/NEA International Stripa Project Overview, Vol. II: Natural Barriers SKB, Stockholm.

Graham, J., Saadat, F., Gray, M.N., 1990. High pressure triaxial

testing on the Canadian reference buffer material. Eng. Geol. 28, 391–403.

Gray, M.N., 1993. OECD/NEA International Stripa Project Overview, Vol. III: Engineered Barriers SKB, Stockholm.

Hueckel, T., Peano, A. (Eds.), 1995. Thermo-Mechanics of Clays and Clay Barriers. Special Issue of Engineering Geology, vol. 41, pp. 1–301.

Huertas, F. et al., 2000. Full-scale engineered barriers experiment for a deep geological repository for high-level radioactive waste in crystalline host rock, European Commission Nuclear Science and Technology, EUR 19147, Brussels.

Ishikawa, H., Amemiya, K., Yusa, Y., Sasaki, N., 1989. Comparison of fundamental properties of Japanese bentonite as buffer material for waste disposal. Proc. 9th Int. Clay Conf. Strasbourg, pp.

Jing, L. et al., 1999. DECOVALEX II Executive Summary, Swedish Nuclear Power Inspectorate, SKI Report 99:24.

Johnson, L.H., LeNeveau, D.M., Shoesmith, D.W., Oscarson, D.W., Gray, M.N., Lemire, R.J. and Garisto, C., 1994. The Disposal of Canada's Nuclear Fuel Waste: The Vault Model for Postclosure Assessment. AECL Research Report, AECL-1071, COG-93-4.

Laughton, A.S., Roberts, L.E.J., Wilkinson, D., Gray, D.A. (Eds.), 1986. The Disposal of Long-Lived and Highly Radioactive Wastes. Proceedings of a Royal Society Discussion Meeting Royal Society, London, p. 189.

Lopez, R.S., 1987. The vault-sealing program, Proceedings of the Workshop, December 1–2, Toronto, Ontario, Atomic Energy of Canada Limited Technical Report TR339.

OECD, 1988. Geological disposal of radioactive wastes: in situ research and investigations in OECD countries: report prepared by NEA Advisory Group, OECD, Paris, France.

Pusch, R. (Ed.), 1990. Artificial Clay Barriers for High Level Radioactive Waste Repositories. Special Issue of Engineering Geology, vol. 28, pp. 230–455.

Radhakrishna, H.S., 1984. Thermal properties of clay-based buffer materials for nuclear waste disposal vault. Atomic Energy of Canada Technical Report, AECL, 7805.

Radhakrishna, H.S., Lau, K.C., Crawford, A.M., 1990. Experimental modeling of the near-field thermal regime in a nuclear waste disposal vault. Special Issue on Artificial Clay Barriers for High Level Radioactive Waste Repositories. Engineering Geology, vol. 28, pp. 337–351.

Selvadurai, A.P.S., 1990. Heat-induced moisture movement within a clay-based sealing material. Special Issue on Artificial Clay Barriers for High Level Radioactive Waste Repositories. Engineering Geology, vol. 28, pp. 325–335.

Selvadurai, A.P.S., 1992. Experimental determination of parameters governing heat-induced moisture movement in a clay buffer. In: Sombret, G.C. (Ed.), Proceedings XVth Symposium on the Scientific Basis for Nuclear Waste Management, Strasbourg. Mater. Res. Soc., vol. 257, pp. 539–545, Boston.

Selvadurai, A.P.S., 1996a. Heat-induced moisture movement in a clay barrier: I. Experimental modelling of borehole emplacement. Eng. Geol. 41, 239–256.

Selvadurai, A.P.S., 1996b. Heat-induced moisture movement in a clay barrier: II. Computational modelling and comparison with experimental results. Eng. Geol. 41, 219–238.

Selvadurai, A.P.S. (Ed.), 1997. Hydro-Thermo-Mechanics of Engineered Clay barriers and Geological Barriers. Special Issue of Engineering Geology, vol. 47, pp. 311–317.

Selvadurai, A.P.S., Cheung, S.C.H., 1991. Hygro-thermal performance of an engineered clay barrier. In: Abrajano, J.T., Johnson, L.H. (Eds.), Scientific Basis for Nuclear Waste Management, MRS Research Symposium, vol. 212, pp. 475–481.

Selvadurai, A.P.S., Onofrei, C., 1993. Hygro-thermal performance of an engineered clay barrier during sustained heating. Proceedings of the International Conference on Nuclear Waste management and Environmental Rehabilitation, Prague, vol. 1, pp. 17–28.

SKI, 1993. DECOVALEX. Mathematical Models of Coupled T-H-M Processes from Nuclear Waste Repositories. Report of Phase 1. Report SKI TR 93:31, Stockholm, Sweden.

Simmons, G.R., Baumgartner, P., 1994. The Disposal of Canada's Nuclear Fuel Waste: Engineering for a Disposal Facility. AECL Research Report, AECL-10715, COG-93-5.

Stephansson, O., Tsang, C.-F., Kautsky, F. (Eds.), 2001. Thermo-Hydro-Mechanical Processes. Special Issue of Int. J. Rock Mech. Mining. Sciences and Geomech. Abstracts, vol. 38, pp. 1–161.

Yong, R.N., Boosinsuk, P., Yiotis, D., 1985. Creep behaviour of a buffer material for nuclear fuel waste vault. Can. Geotech. J. 22, 541–550.

Yong, R.N., Boosinsuk, P., Wong, G., 1986. Formulation of backfill material for a nuclear fuel waste disposal vault. Can. Geotech. J. 23, 216–228.

Yong, R.N., Mohamed, A.M.O., Xu, D.M., 1990. Coupled heat–mass transport effects on moisture redistribution prediction in clay barriers. Eng. Geol. 28, 315–324.